Influence of two-body and three-body interatomic forces on gas, liquid, and solid phases

Liping Wang and Richard J. Sadus*
Centre for Molecular Simulation, Swinburne University of Technology, PO Box 218 Hawthorn, Victoria 3122, Australia
(Received 6 June 2006; published 25 August 2006)

Accurate molecular dynamics simulations are reported which quantify the contributions of two- and three-body interactions in the gas, liquid, and solid phases of argon at both subcritical and supercritical conditions. The calculations use an accurate two-body potential in addition to contributions from three-body dispersion interactions from third-order triple-dipole interactions. The number dependence of three-body interactions is quantified, indicating that a system size of at least five hundred atoms is required for reliable calculations. The results indicate that, although the contribution of three-body interaction to the overall energy is small, three-body interactions significantly affect the pressure at which vapor-liquid and solid-liquid transitions are observed. In particular, three-body interactions substantially increase the pressure of the freezing point. Unlike two-body interactions, which vary with both density and temperature, for a given density, three-body interactions have a near-constant 'background' value irrespective of the temperature. Both two-body interactions and kinetic energy have an important role in vapor-liquid equilibria whereas solid-liquid equilibria are dominated by two-body interactions.

DOI: 10.1103/PhysRevE.74.021202 PACS number(s): 61.20.Ja, 68.18.Jk, 82.20.Wt, 34.20.Cf

I. INTRODUCTION

Molecular simulation [1] studies routinely evaluate pairwise interactions via an effective multibody intermolecular potential such as the Lennard-Jones potential. The use of effective multibody potentials provides a practical method for calculating the physical properties of materials at a reasonable computational cost. In contrast, the addition of three- or more-body interactions remains computationally prohibitive, despite improvements in algorithms and parallel computing [2]. However, the use of effective intermolecular potentials hides the physics involved in multibody interactions. In the absence of external forces, the contribution of multibody interactions to energy can be obtained as the infinite sum of two-, three-, four-, and higher-body interactions. Fortunately, the magnitude [1] of successive contributions declines rapidly and their signs alternate, which means that there is a high degree of cancellation. Therefore, it is likely that the combination of two-body and three-body interactions is a very good approximation of the total sum of multibody interactions. It has been documented [3–5] that three-body interactions can make a small but significant contribution to the energy of liquids. For example, recent work [6–11] involving either the use of an accurate two-body potential in combination with a three-body potential [6,7] or *ab initio* intermolecular potentials [8–11], has demonstrated that the vapor-liquid equilibria of pure fluids are quite sensitive to three-body interactions.

The aim of this work is to isolate and quantify the contribution of two- and three-body interactions in gas, liquid, and solid phases. Molecular dynamics simulations were performed using accurate two-body and three-body intermolecular potentials, covering a wide range of density at both subcritical and supercritical conditions. The results can be used to evaluate the role of two- and three-body interactions both on vapor-liquid and solid-liquid equilibria.

*Email address: RSadus@swin.edu.au

II. THEORY

A. Intermolecular potentials

Two-body interactions are undoubtedly the dominant influence on the properties of fluids. Therefore, an accurate description of two-body interactions is required before any conclusions concerning the influence of three-body interaction can be made reliably. This important pre-condition severely limits the scope of systems that can be investigated. In practice, this means that we are limited to noble gases for which accurate two-body potentials are available. Although *ab initio* two-body potentials are available for some diatomic systems such as hydrogen and nitrogen, they are generally of lesser quality than noble gas potentials. Details of the intermolecular potentials have been discussed elsewhere [7] and therefore only a brief outline is given here. The two-body interactions of argon are well represented by the Barker-Fisher-Watts (BFW) potential [12] which is a linear combination of the Barker-Pompe [13] (u_{BP}) and Bobetic-Barker [14] (u_{BB}) potentials

$$u_2(r) = 0.75u_{\mathrm{BB}}(r) + 0.25u_{\mathrm{BP}}(r), \tag{1}$$

where the potentials of Barker-Pompe and Bobetic-Barker have the following form:

$$u_2(r) = \epsilon\left[\sum_{i=0}^{5} A_i(z-1)^i \exp[\alpha(1-z)] - \sum_{j=0}^{2} \frac{C_{2j+6}}{\delta + z^{2j+6}}\right]. \tag{2}$$

In Eq. (2), $z=r/r_m$ where r_m is the intermolecular separation at which the potential has a minimum value and the other parameters are obtained by fitting the potential to experimental data for molecular beam scattering, second virial coefficients, and long-range interaction coefficients. The contribution from repulsion has an exponential dependence on intermolecular separation and the contribution to dispersion of the C_6, C_8, and C_{10} coefficients are included. The only difference between the Barker-Pompe and Bobetic-Barker potentials is that a different set of parameters is used in each

case. The values of these parameters [12] are summarized in Table I.

Different types of interaction are possible depending on the distribution of multipole moments between the atoms [15–17]. Marcelli and Sadus [7] evaluated the contributions from third-order interactions involving dipoles and quadrupoles in addition to the fourth-order triple dipole contribution. There is a high degree of cancellation of the multipole terms, which means that the third-order triple dipole term alone is a good representation of three-body dispersion interactions. Bukowski and Szalewicz [18] have reported *ab initio* calculations for phase behavior of argon, which also demonstrate that the total three-body nonadditive effect can be largely attributed to triple dipole interactions. In view of this, we have only considered contributions from third-order triple-dipole interactions in this work.

The triple-dipole potential can be evaluated from the formula proposed by Axilrod and Teller (AT) [19]:

$$u_{DDD}(ijk) = \frac{\upsilon_{DDD}(ijk)(1 + 3\cos\theta_i \cos\theta_j \cos\theta_k)}{(r_{ij}r_{ik}r_{jk})^3} \quad (3)$$

where $\upsilon_{DDD}(ijk)$ is the nonadditive coefficient [20], and the angles and intermolecular separations refer to a triangular configuration of atoms.

B. Simulation details

NVT molecular dynamics simulations were performed for 108, 256, 500, and 864 argon atoms at different temperatures and reduced densities ranging from 0.03 to 1.3. The starting structure was a face centered cubic lattice. The equations of motion were integrated by a fourth order Gear predictor-corrector scheme [1] with a reduced integration time step of 0.001. The first 50 000 time steps of each trajectory were used to equilibrate the system, and a further 200 000 time steps were carried out to calculate average values. Adopting the common practice of molecular simulation, the temperature ($T^* = k_B T/\epsilon$), density ($\rho^* = \rho\sigma^3$, where σ is the distance at which the two-body potential has a value of zero), pressure ($p^* = p\sigma^3/\epsilon$), and energy ($E^* = E/\epsilon N$) are reported in reduced units relative to the intermolecular parameters of the BFW potential.

Periodic boundary conditions were applied. The BFW two-body potential was truncated at half the box length and long-range corrections were used to recover the full contribution to the intermolecular potential. A cutoff distance of a quarter of the box length was used for three-body interactions from the AT potential. It is very well known that, for periodic systems involving pairwise interactions, the cut-off distance for the simulation must not exceed half of the box length. However, as discussed elsewhere [7], when three-body interactions are involved the cutoff distance for the three-body term must not exceed a quarter of the box length. If this distance is exceeded, the triplets obtained will not be correctly imaged. Three-body calculations were only performed when all three intermolecular separations were within the cutoff distance and long-range corrections were not used. A feature of the calculations reported here is that contributions of two- and three-body interactions to both energy and pressure were obtained accurately. The standard errors in the energies and pressures were typically both less than 0.1%.

TABLE I. Summary of the intermolecular potential parameters used in this work.

	Argon[a]	
υ_{DDD}(a.u.)[b]	518.3	
ϵ/k(K)	142.095	
σ (Å)	3.3605	
r_m(Å)	3.7612	
	Barker-Pompe	Bobetic-Barker
α	12.5	12.5
δ	0.01	0.01
A_0	0.2349	0.29214
A_1	−4.7735	−4.41458
A_2	−10.2194	−7.70182
A_3	−5.2905	−31.9293
A_4	0.0	−136.026
A_5	0.0	−151.0
C_6	1.0698	1.11976
C_8	0.1642	0.171551
C_{10}	0.0132	0.013748

[a]Two-body parameters from Ref. [12].
[b]From Ref. [20].

III. RESULTS AND DISCUSSION

A. Influence of system size

The effect of system size on properties obtained from pairwise interactions is well known [1]. In contrast, we are not aware of any systematic investigation of the system-size dependency of three-body interactions. Figure 1(a) illustrates the two-body energy obtained for systems of 108, 256, 500, and 864 atoms at densities covering gas, liquid, and solid phases. The discontinuity in the energy signifies the occurrence of solid-liquid phase transition. The relative percentage differences of two-body energies with respect to the largest system are presented in Fig. 1(b), which indicates that the largest deviations occur at either low or high densities. In between these extremes, the effect of system size is largely independent of density. For most practical purposes, a system size of 500 atoms is sufficient to obtain reasonable results.

The effect of system size on three-body energies is illustrated in Fig. 2. Comparing the data in Fig. 2 with the corresponding data in Fig. 1, it appears that the size of the system has a much greater influence on three-body energy than on two-body energy. In particular, the three-body energy obtained for 108 atoms display very large deviations from the results obtained for larger number of atoms. Furthermore, the difference in the 256 atom calculations relative to calculations with either 500 or 864 atoms is much larger than the corresponding two-body calculations. A possible explanation for these discrepancies is that, for small systems, signifi-

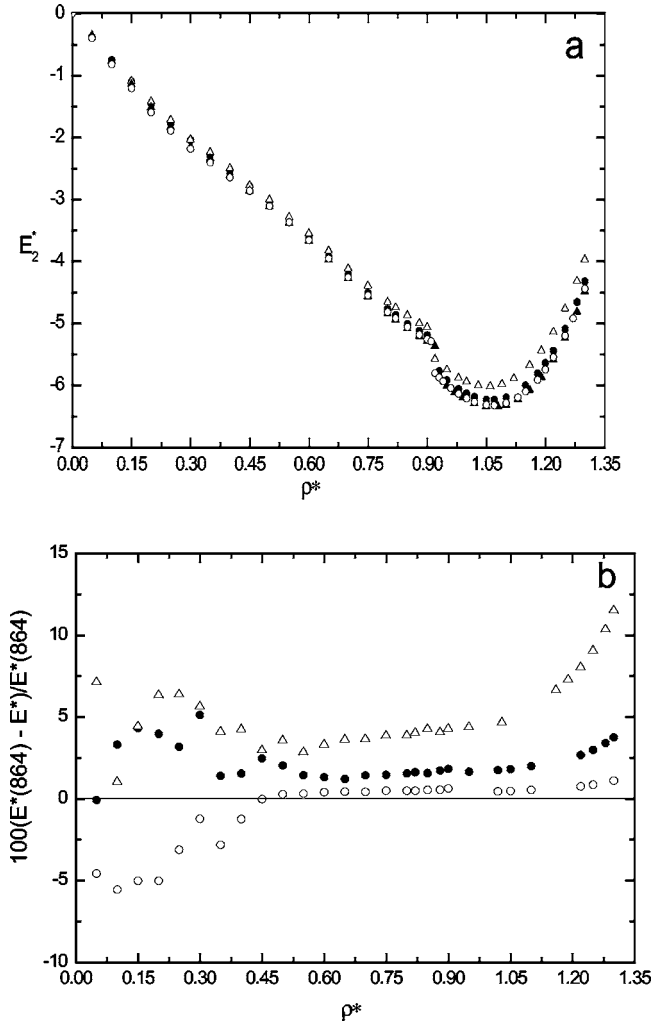

FIG. 1. (a) Comparison of two-body potential energies obtained for ensembles with different numbers of argon atoms (△108, ●256, ○500, and ▲864) at different densities and $T^*=0.9914$. (b) Relative percentage difference between two-body potential energy of different system size and that of 864 argon atoms.

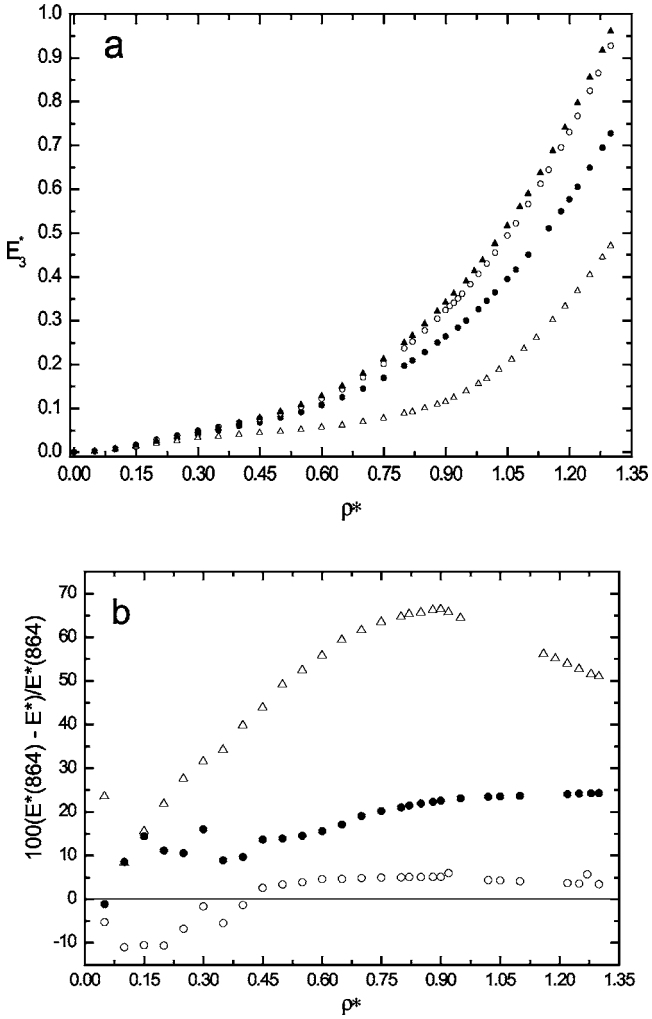

FIG. 2. (a) Comparison of three-body potential energies obtained for ensembles with different numbers of argon atoms (△108, ●256, ○500, and ▲864) at different densities and $T^*=0.9914$. (b) Relative percentage difference between three-body potential energy of different system size and that of 864 argon atoms.

cantly fewer triplets are encountered within the cutoff distance. In view of this, a system size of 500 atoms appears to be the minimum requirement to obtain reasonably accurate results. We note that to minimize computation time, three-body simulations have been reported previously in the literature with fewer than 500 atoms. In some cases, the conclusions reached in these earlier simulations may need to be revised to account for the significant influence of system size on three-body interactions.

The effect of system size on the total potential energy is illustrated in Fig. 3(a). In this case, the size dependency of the results is relatively small. The relative percentage differences of the total potential energies are shown in Fig. 3(b). At medium to high densities the relative deviations of the total potential energy are small both in absolute terms and in comparison with either the deviations observed for two-body or three-body energies. This indicates that, to some extent, the fluctuations of two-body and three-body potential energies with system size cancel each other at medium densities. Indeed, the system size dependence of the two-body + three body potential is similar to that exhibited by effective multibody potentials such as the Lennard-Jones potential. In view of these considerations, a system size of 500 atoms represents a reasonable compromise between the need to minimize both system size effects and the large computational cost involved in performing three-body calculations.

B. Two- and three-body effects at subcritical temperatures

To study the effects of two- and three-body interactions on gas, liquid, and solid phases, we initially performed simulations at a subcritical temperature ($T^*=0.9914$) for which both vapor-liquid and solid-liquid equilibria could be expected at appropriate densities. Simulations at $T^*=0.9914$ with reduced densities ranging from 0.03 to 1.3 are summarized in Figs. 4–6.

The contributions of two- and three-body interactions to the potential energy are illustrated in Fig. 4(a). At all densities, three-body interactions make a positive contribution to

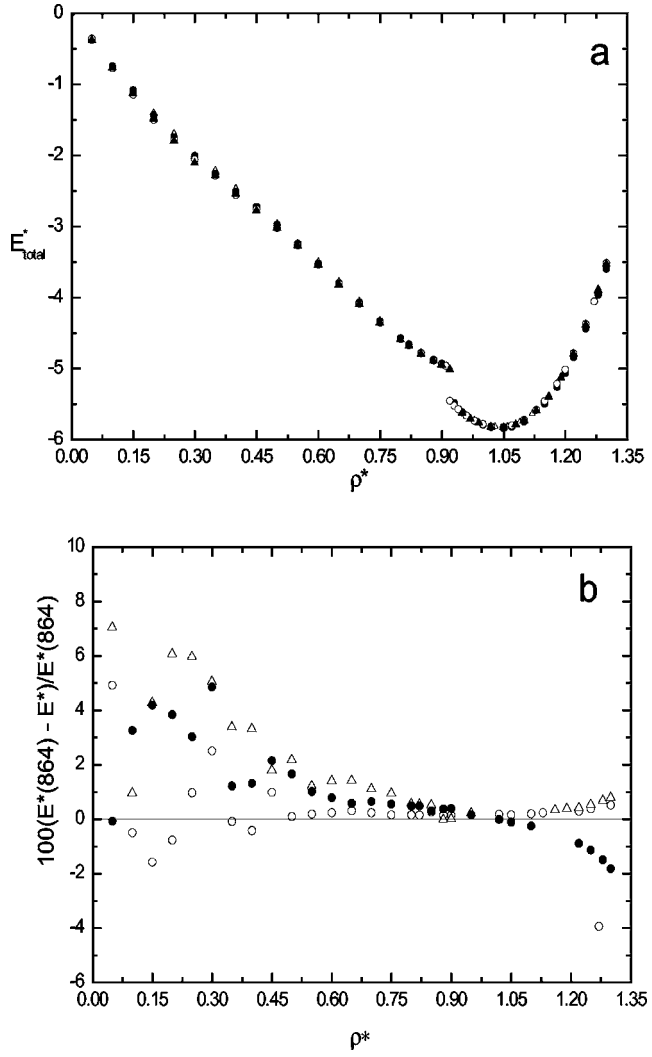

FIG. 3. (a) Comparison of the total potential energies obtained for ensembles with different numbers of argon atoms (△108, ●256, ○500, and ▲864) at different densities and $T^*=0.9914$. (b) Relative percentage difference between total potential energy of different system size and that of 864 atom system of argon.

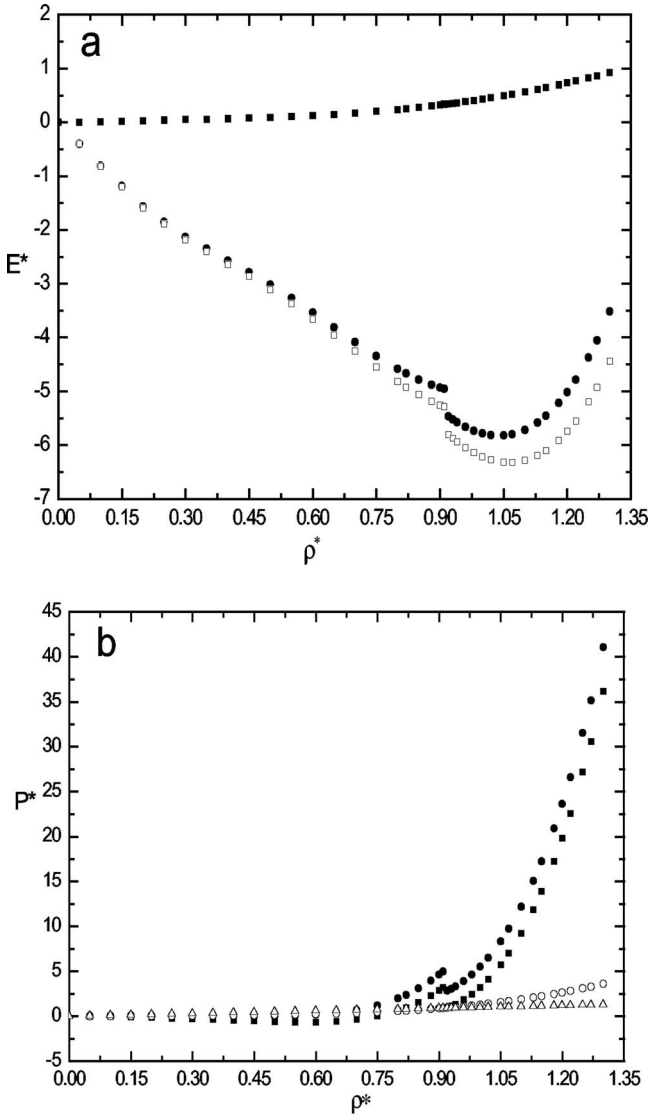

FIG. 4. Comparison of (a) potential energies [□E^*_2, ■E^*_3, and ● ($E^*=E^*_2+E^*_3$)] and (b) pressures (●P^*_{total}, ■P^*_2, ○P^*_3, and △P^*_k) calculated for a system of 500 argon atoms at different densities with $T^*=0.9914$.

the energy, which progressively increases with increasing density. In contrast, Fig. 4(a) shows that the contribution of two-body energy is always negative and it steadily declines (i.e., it becomes more negative) with increasing vapor, liquid, or metastable fluid densities. A discontinuity in the two-body energy is observed in the vicinity of the solid-liquid transition. The formation of a face-centered cubic (fcc) solid was observed. As discussed below, it should be noted that this discontinuity is not the exact location of the freezing point because it is likely that both the liquid and solid curves extend partly into metastable regions. At densities immediately after the solid-liquid transition, the two-body energy initially declines further, following the trend observed in the vapor and liquid phases. However, at higher densities ($\rho^*>1.1$), this trend is reversed and the two-body energy of the solid phase becomes progressively larger (i.e., it becomes less negative). The trend in the total potential energy mirrors the trend in the two-body energy. The effect of three-body interactions is to shift the overall energy to higher values. This effect is hardly noticeable in the vapor and liquid regions but it is quite significant in the solid phase.

The contributions of two- and three-body interactions to the pressure are illustrated in Fig. 4(b). The contribution of the kinetic term to pressure is also given for comparison. Two-body interactions make a negative contribution to pressure at all vapor and liquid phase densities ($\rho^*=0.03-0.70$). However, in the solid phase, the two-body pressure is positive and it increases rapidly with increasing density. In contrast, the three-body pressure has a positive value at all densities and its contribution steadily increases with density. Although two-body interactions have the dominant influence, the contributions of three-body interactions in the liquid phase are important in achieving a positive overall pressure. Furthermore, when $\rho^*>0.91$, the three-body pressure exceeds the contribution of the kinetic term and it completely

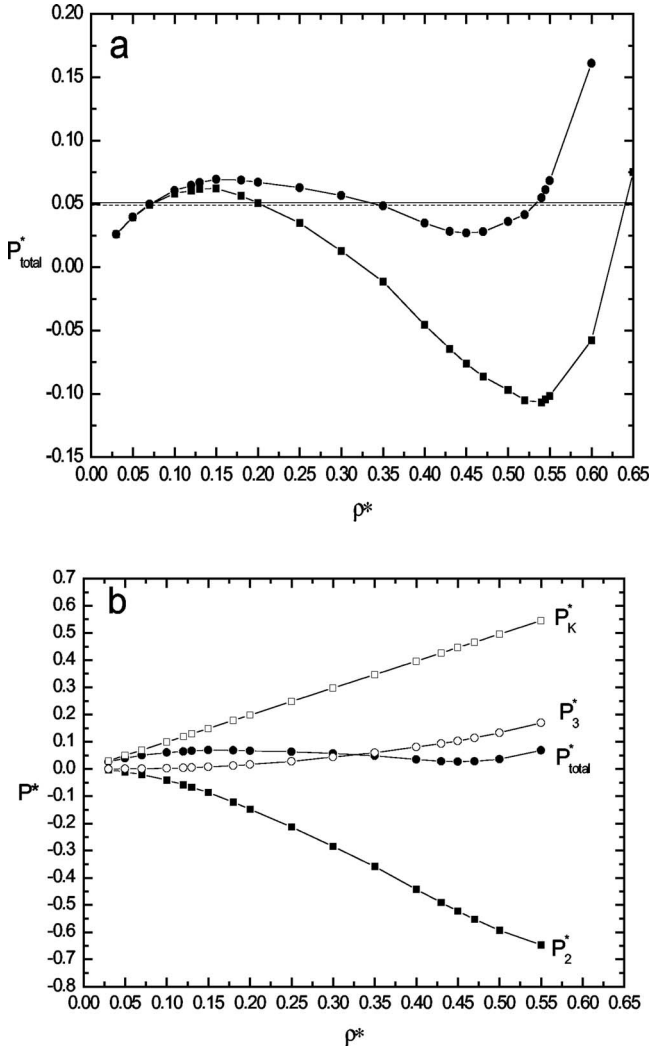

FIG. 5. (a) The total pressure ($P^*_{\text{total}}=P^*_2+P^*_3P^*_k$) (-●-) and ($P^*_2+P^*_k$) (-■-) at $T^*=0.9914$ from simulations for 500 argon atoms between the liquid and vapor coexistence densities. The pressures display "van der Waals" loops in the two-phase vapor-liquid region. The equilibrium coexisting pressures for the two cases (dotted and solid lines) were obtained from Gibbs ensemble simulations. (b) Comparison of the various contributions to pressure.

dominates the kinetic term in the solid phase. Indeed, at very high densities, neglecting the kinetic term and simply combining the two- and three-body terms makes a good approximation for the total pressure.

Figure 5 illustrates the pressure of the vapor and liquid regions of the system in greater detail. A vapor-liquid phase transition is evident from the "van der Waals loop" [21]. Initially, the pressure increases with the increasing of density. When $\rho^*=0.15$, the pressure begins to decline, signaling the beginning of a two-phase region of vapor and liquid coexistence. The decline in pressure is subsequently reversed at higher densities and a single-phase liquid branch is formed. The van der Waals loop is observed both in analytical equations of state and molecular simulations. It represents a metastable extension of the liquid and vapor branches inside of the two-phase region. The van der Waals loop is not observed in real systems, which display a discontinuity at the

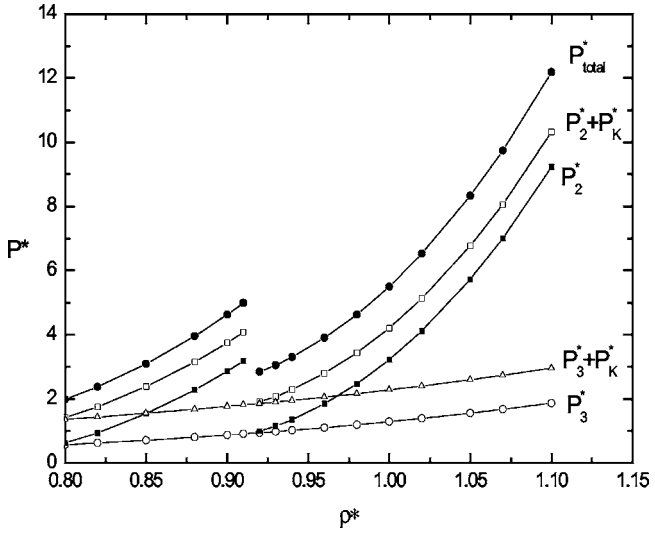

FIG. 6. Comparison of the various contributions to pressure in the vicinity of the solid-liquid phase transition from simulations for 500 argon atoms at $T^*=0.9914$.

equilibrium pressure. The equilibrium pressure can be obtained by using the "Maxwell rule" [21]. At equilibrium, an isobar passing through the van der Waals loop will result in two regions, above and below the isobar, which must be of equal area. If a sufficiently large number of particles are used in the simulation, the van der Waals loop vanishes [22], which is consistent with experiment. Although it can be argued that the van der Waals loop observed in molecular simulations is most commonly an artifact, it nonetheless serves the useful purpose of signaling a phase transition in conventional simulations.

The van der Waals loops obtained from simulations using the total pressure (two-body+three-body+kinetic terms) and simply the sum of the kinetic and two-body terms are compared in Fig. 5(a). It is apparent from this comparison, that excluding three-body interactions has a large influence on the shape and size of the van der Waals loop. In particular, the liquid-side turning point occurs at considerably lower pressures and the region of two-phase coexistence is increased considerably. The change in the size of the two-phase region is consistent with simulations reported elsewhere [6,7] for two- and three-body interactions. However, it is also apparent that application of the equal area rule to the two different van der Waals loops would result in substantially different coexistence pressures. For the two cases, the coexistence properties were determined independently using the *NVT*-Gibbs ensemble [23] algorithm. It is apparent from Fig. 5(a) that an isobar obtained using the coexistence pressure form Gibbs ensemble simulations that include two-body+three-body+kinetic terms cuts the corresponding van der Waals loop into two equal portions. In contrast, when Gibbs ensemble simulations were performed using only two-body interactions and the ideal gas term, the coexistence liquid phase density changes substantially, but the pressure is only slightly lowered. It is apparent from Fig. 5(a) that the small change in coexistence pressure is inconsistent with the application of the Maxwell equal area rule for the second van der Waals loop, which requires a substantially lower, even nega-

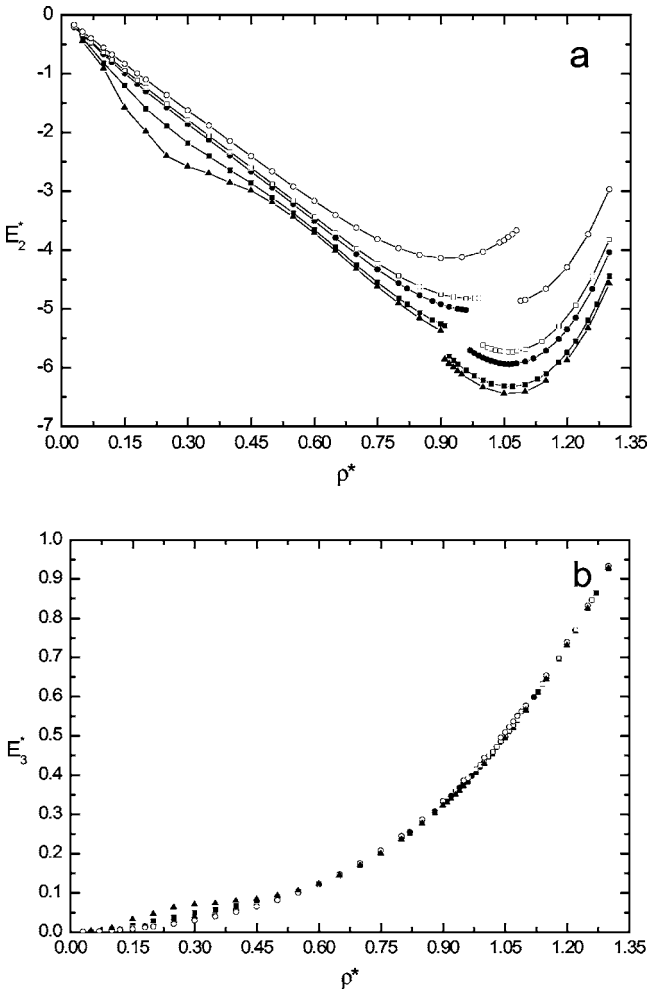

FIG. 7. (a) Two-body and (b) three-body potential energies as a function of density at different temperatures. Results are shown for subcritical [$T^*=0.9$(▲), $T^*=0.9914$(■)], near critical [$T^*=1.2678$(●)], and supercritical [$T^*=1.4168$(□), $T^*=2.0$(○)] temperatures.

tive pressure. This illustrates the fact that the van der Waals loop is an artifact and that the Maxwell rule does not necessarily apply to all simulation results. In particular, it appears that the valid use of the Maxwell rule requires simulations to include interactions other than two-body interactions such as in the Lennard-Jones potential.

The various contributions to pressure at densities covering the transition between vapor and liquid phases are examined in Fig. 5(b). The contribution of three-body interactions to the pressure slowly increases from the vapor, vapor and liquid, and liquid phase regions. However, the contributions of the two-body and kinetic terms are of more significance to the behavior of the system. Starting from the vapor phase, the two-body and kinetic contributions begin to diverge rapidly in opposite directions. The change in the kinetic contribution with respect to density is more uniform but less rapid than the two-body term. These subtle differences in behavior are significant because it means that the two contributions do not cancel but instead result in the van der Waals loop. This suggests that the two-phase vapor-liquid region depends on the interplay between two-body interactions and kinetic forces. In the absence of either a kinetic term or two-body interactions, only a single phase would be observed. The role of three-body interactions is primarily to reduce the size of the two-phase region and to increase the coexistence pressure.

Figure 6 shows the effect of various components of pressure in the vicinity of the solid-liquid transition. The vicinity of the solid-liquid transition is marked by a discontinuity in the pressure-density behavior. A complete van der Waals loop is not commonly observed for the solid-liquid transition but the same considerations apply. The liquid and solid branches extend into metastable regions, which means that the coexistence pressure occurs at a pressure somewhat below maximum pressure of the liquid branch. Three-body interactions make a significant contribution to the pressure of both the liquid and solid phases. Neither three-body interactions alone nor the combination of three-body interactions and the kinetic term can cause a solid-liquid phase transition. In contrast, two-body interactions appear to have the controlling influence on the liquid-solid phase transition. The effect of the kinetic contribution and three-body interactions is to shift the solid-liquid phase transition to lower densities and substantially higher pressure. The two-body interactions include a contribution from repulsive interaction, which probably has the dominant influence. This is consistent with the observation of a solid-liquid transition for purely repulsive hard spheres [1,24,25]. It also highlights the difference between vapor-liquid and solid-liquid equilibria. A two-phase vapor-liquid region is formed as the consequence of the interplay of two-body interactions and the kinetic term whereas two-body interactions have the dominant influence in causing the separation into liquid and solid phases.

C. Interatomic forces at different temperatures

The two- and three-body intermolecular potentials involve only terms that are independent of temperature. Nonetheless, the contributions from two- and three-body interactions can be expected to vary with temperature because temperature affects the interatomic separations. In Figs. 7 and 8, we report results for temperatures that are subcritical ($T^*=0.9$ and $T^*=0.9914$), near critical ($T^*=1.2678$), and supercritical ($T^*=1.4168$ and $T^*=2.0$).

The contributions of two- and three-body interactions to the energy of the system at various temperatures are illustrated in Figs. 7(a) and 7(b), respectively. It is apparent from Fig. 7(a) that the contribution of two-body interactions to energy varies significantly with temperature. In general, for any given density, the two-body contribution to energy increases (i.e., it becomes less negative) as the temperature increases. At $T^*=0.9$ a pronounced dip in the energy-density behavior is observed at low densities, which corresponds to the region of two-phase coexistence. This is in part due a more pronounced van der Waals loop that is often associated with phase coexistence at lower temperatures [21]. At supercritical temperatures ($T^*=2.0$), the liquid branch of the curve begins to turn-upwards at lower densities. In contrast to two-body interactions, the data in Fig. 7(b) indicate that the contribution of three-body interactions to energy remains largely

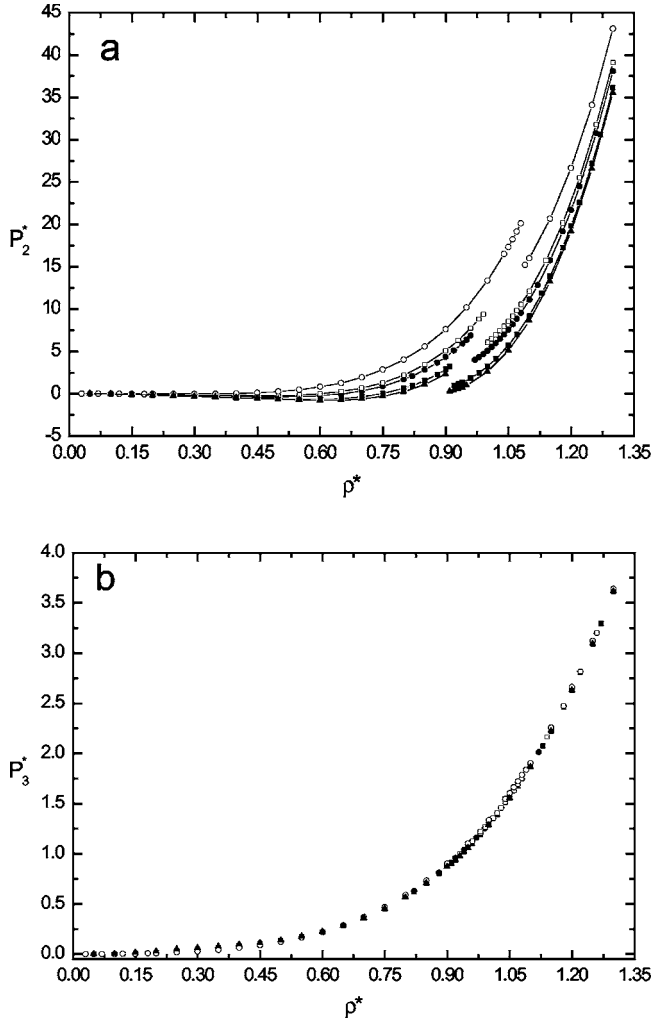

FIG. 8. (a) Two-body and (b) three-body pressures as a function of density at different temperatures. Results are shown for subcritical [$T^*=0.9$(▲), $T^*=0.9914$(■)], near critical [$T^*=1.2678$(●)], and supercritical [$T^*=1.4168$(□), $T^*=2.0$(○)] temperatures.

constant irrespective of the temperature. This probably reflects the fact that three-body interactions are very short-ranged and relatively small variations in temperature do not significantly affect the number of triplets that are within range of the AT potential.

The contributions of two- and three-body interactions to the pressure of the system at various temperatures are illustrated in Figs. 8(a) and 8(b), respectively. The main effect [Fig. 8(a)] of increasing temperature is to considerably increase the two-body pressure in the vicinity of the solid-liquid phase transition. In common with the three-body energy, the three-body contribution to pressure [Fig. 8(b)] remains largely constant irrespective of temperature.

The calculations did not include the effects of three-body repulsion. The effect of three-body repulsion could at least partially offset the influence of the AT term. Our knowledge of three-body interactions is currently quite limited [1]. In any case, under normal conditions, the number of triplets that would be in sufficiently close proximity to each other for three-body repulsion to have a significant influence is likely to be very small. The insensitivity of three-body interactions to temperature indirectly supports this inference. Three-body dispersion occurs over a much larger range of interatomic separations than three-body repulsion but despite this, changes in temperature did not affect the magnitude of their contribution. Therefore, the effect of three-body repulsion is likely to be limited to very high pressures and very high densities. Outside of such extreme conditions, two-body repulsion is likely to be a very good approximation of the overall repulsion. In the absence of a significant contribution from three-body repulsion, it has been demonstrated [26] that accurate two-body potentials can be used in conjunction with an interpolation formula for three-body interactions.

Although argon has been the focus of this work, the conclusions reached here are equally valid for other noble gases such as krypton and xenon and we would expect them to generally apply to nonpolar molecules. To test this, we partly repeated the analysis for krypton and xenon. The krypton and xenon calculations required modifications to the BFW potential as described elsewhere [3]. The results for both krypton and xenon were qualitatively very similar to the argon results.

IV. CONCLUSIONS

To accurately determine the contribution of three-body interactions, a system size of at least 500 atoms is required. The contribution of three-body interactions increases progressively with density. At subcritical temperatures, three-body interactions can be expected to dominate the contribution of the kinetic term in the solid phase. The occurrence of vapor-liquid equilibria can be attributed to the interplay between two-body interaction and the kinetic term. In contrast, two-body interactions are the controlling influence on solid-liquid equilibria. However, the inclusion of three-body interactions results in a substantial increase in pressure, particularly for the solid phase. The contribution of two-body interactions varies considerably with temperature whereas three-body interactions remain largely constant irrespective of temperature. This means that for a given density, three-body interactions have a near-constant "background" influence at all temperatures. The application of the Maxwell rule for determining the coexistence pressure appears to require the inclusion of three-body interactions or the use of effective intermolecular potentials. Although the calculations were confined to the specific case of the noble gases, the conclusions reached are likely to apply to materials in general.

ACKNOWLEDGMENTS

L.W. thanks the Australian government for financial assistance. The Australian Partnership for Advanced Computing provided a generous allocation of computer time.

[1] R. J. Sadus, *Molecular Simulation of Fluids: Theory, Algorithms and Object-Orientation* (Elsevier, Amsterdam, 1999).
[2] J. Li, Z. Zhou, and R. J. Sadus, Comput. Phys. Commun. (to be published).
[3] J. A. Barker, R. O. Watts, J. K. Lee, T. P. Schafer, and Y. T. Lee, J. Phys. Chem. **61**, 3081 (1974).
[4] A. Monson, M. Rigby, and W. A. Steele, Mol. Phys. **49**, 893 (1983).
[5] M. J. Elrod and R. J. Saykally, Chem. Rev. (Washington, D.C.) **94**, 1975 (1994).
[6] J. A. Anta, E. Lomba, and M. Lombardero, Phys. Rev. E **55**, 2707 (1997).
[7] G. Marcelli and R. J. Sadus, J. Chem. Phys. **111**, 1533 (1999).
[8] P. S. Vogt, R. Liapine, B. Kirchner, A. J. Dyson, H. Huber, G. Marcelli, and R. J. Sadus, Phys. Chem. Chem. Phys. **3**, 1297 (2001).
[9] G. Raabe and R. J. Sadus, J. Chem. Phys. **119**, 6691 (2003).
[10] A. E. Nasrabad and U. K. Deiters, J. Chem. Phys. **119**, 947 (2003).
[11] A. E. Nasrabad, R. Laghaei, and U. K. Deiters, J. Chem. Phys. **121**, 6423 (2004).
[12] J. A. Barker, R. A. Fisher, and R. O. Watts, Mol. Phys. **21**, 657 (1971).
[13] J. A. Barker and A. Pompe, Aust. J. Chem. **21**, 1683 (1968).
[14] M. V. Bobetic and J. A. Barker, Phys. Rev. B **2**, 4169 (1970).
[15] W. L. Bade, J. Chem. Phys. **28**, 282 (1958).
[16] R. J. Bell, J. Phys. B **3**, 751 (1970).
[17] M. B. Doran and I. J. Zucker, J. Phys. C **4**, 307 (1971).
[18] R. Bukowski and K. Szalewicz, J. Chem. Phys. **114**, 9518 (2001).
[19] B. M. Axilrod and E. Teller, J. Chem. Phys. **11**, 299 (1943).
[20] P. J. Leonard and J. A. Barker, in *Theoretical Chemistry: Advances and Perspectives*, edited by H. Eyring and D. Henderson (Academic Press, London, 1975), Vol. 1.
[21] I. Prigogine and R. Defay, *Chemical Thermodynamics*, edited by D. H. Everett (Longams, Green and Co., London, 1954).
[22] R. Yamamoto, O. Kitao, and K. Nakanishi, Mol. Phys. **84**, 757 (1995).
[23] A. Z. Panagiotopoulos, N. Quirke, M. Stapleton, and D. J. Tildesley, Mol. Phys. **63**, 527 (1988).
[24] B. J. Alder and T. E. Wainwright, J. Chem. Phys. **27**, 1208 (1957).
[25] G.-W. Wu and R. J. Sadus, AIChE J. **51**, 309 (2005).
[26] G. Marcelli and R. J. Sadus, J. Chem. Phys. **112**, 6382 (2000).